BRUKER

Application Note
#156

Characterizing Ferroelectric Materials with SS-PFM and DCUBE PFM

Piezoresponse force microscopy (PFM) is a powerful technique for studying ferroelectric materials due to the high sensitivity and nanometer-level resolution that it inherits from atomic force microscopy (AFM). PFM-based spectroscopic methods, such as switching spectroscopy PFM (SS-PFM) and DataCube™ PFM (DCUBE PFM), allow characterization of key parameters of ferroelectrics, such as coercive voltages, nucleation voltages, saturation responses, and more. Unfortunately, quantification and interpretation of PFM results can be complicated by artifacts. In this application note, we discuss the best modes and practices for optimizing PFM measurements to achieve reliable results.

PFM has many variants optimized to solve different problems and study different aspects of electromechanical response (Table 1). This application note focuses on the DCUBE PFM and SS-PFM modes and how they can help with many of these issues. Additionally, the benefits of both resonance and sub-resonance PFM are discussed along with how laser position can be optimized to improve measurement accuracy.

PFM Mode/Method	Benefits
Sub-resonance PFM with laser at electrostatic blind spot	Eliminates electrostatics, simple calibration
Sub-resonance PFM with laser at tip	No need to position laser at ESBS, simple calibration
Contact Resonance PFM	Significant PFM signal amplification, but must consider CR shape factor for quantitative measurements
Contact Mode PFM	Fast and simple especially for sub-resonance PFM
DCUBE PFM mapping	Minimizes tip wear and sample damage, simultaneous mapping of PFM response and mechanical properties such as modulus & adhesion, works with either contact resonance or sub-resonance PFM
SS-PFM spectroscopy and mapping	Same as DCUBE, but additionally allows separation of read and write segments, and use of multiple read segments at different voltages for cKPFM and PFM spectroscopy
Vector PFM (vertical and lateral)	Characterize different components of piezoelectric response tensor
High Voltage PFM	Switch samples with high coercive voltages and/or measure low-response samples
PFM Lithography	Control ferroelectric domain structure and/or investigate domain wall propagation

Table 1

AFM modes and methods for PFM.

Background

To investigate the electromechanical response of materials with PFM, a sinusoidal (AC) drive voltage is applied between a conductive AFM probe and the sample substrate. The inverse piezoelectric effect then causes the sample to expand and contract sinusoidally, which is detected by an AFM probe tip in contact with the sample.

For materials with a positive electrostrictive coefficient, such as lead zirconate titanate (PZT), the sample expands when the polarization of a piezoelectric domain beneath the tip is parallel to an increasing electric field (and vice versa). When the sample expands, the AFM tip is displaced and the cantilever bends, producing a sinusoidal signal in deflection at the same frequency as the AC drive voltage (Figure 1a). It is worth noting that some piezoelectric materials, such as polyvinylidene difluoride (PVDF), have negative electrostrictive coefficients, inverting the previous discussion.

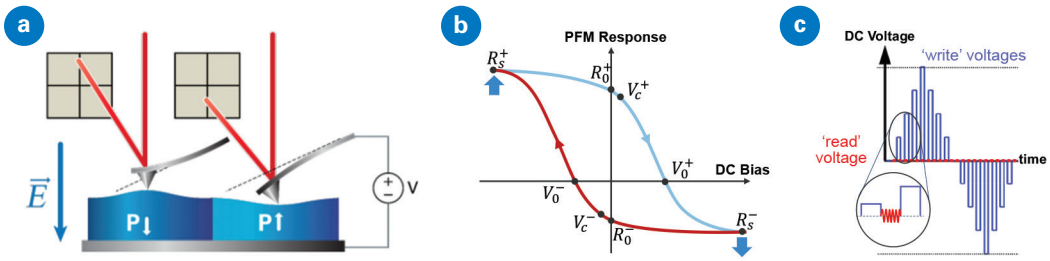

FIGURE 1

Piezoresponse Force Microscopy (PFM) basics: (a) an increasing electric field in parallel with the polarization of a piezoelectric sample will cause the sample to expand if the material has a positive electrostrictive coefficient, (b) a typical hysteresis loop describing the response and domain switching characteristics of a ferroelectric material, and (c) a series of read and write pulses applied during switching spectroscopy PFM (SS-PFM). The write segments use successively larger (or smaller) DC voltages to switch the polarity of the domain beneath the tip, while an AC voltage is applied during read segments allow observation of the polarization and response of the domain after switching.

Since the AFM can measure deflection normal to the sample surface or parallel to the surface (perpendicular to the cantilever), it is possible to simultaneously measure two orthogonal components of the piezoelectric displacement vector. Rotating the sample by 90° can provide the third component, allowing full characterization of the displacement vector.[1]

If the material is ferroelectric, a large enough applied voltage (called the coercive bias) can cause the domain polarization to flip. The new polarization is then maintained after the voltage is removed. Figure 1b depicts a typical ferroelectric hysteresis loop for a material like PZT with a positive electrostrictive coefficient. Key parameters in the loop include coercive voltages ($V_0^{\pm}$), nucleation voltages ($V_c^{\pm}$), remnant responses ($R_0^{\pm}$), and saturation responses ($R_S^{\pm}$). The local measurement of these hysteresis loops and associated parameters is the goal of PFM spectroscopy.[2]

Switching spectroscopy PFM (SS-PFM) improves on the accuracy of PFM spectroscopy by separating measurements of the PFM response during *read voltages* from those during *write voltages* (see Figure 1c).[3] In its simplest form, the AC voltage is turned off during each *write* segment, and then turned back on during each *read* segment to study the stability of domains after poling.

Quantitative PFM makes possible the validation of results using different probes and by other labs. However, there are challenges related to conducting quality PFM measurements:

- Signal levels are often quite small (<10 pm/V), making detection difficult.
- PFM is sensitive to several different types of electromechanical response of the sample, which can be difficult to separate.[4]

- The observed signal is influenced by the measurement system (AFM and probe) in addition to the sample. For example, electrostatic forces between cantilever and surface or background signals from within the AFM can result in a response similar to that of a piezoelectric material.[5]
- PFM results can be inconsistent if the tip or sample is damaged by the uncontrolled lateral forces that occur during contact mode scanning (the traditional mode for PFM scanning).

Maximizing Sensitivity

The signal levels in PFM are generally very small, with typical amplitudes <10 pm/V. This is close to the limit of what an AFM can detect. To address this, one of four approaches are generally taken:

1. Increase the AC stimulation voltage

Since the PFM amplitude is proportional to the AC stimulation voltage (to a first order approximation), doubling the AC voltage will approximately double the PFM response. However, arbitrarily increasing the AC stimulation voltage is not a generally practical approach. Many samples have weak points where leakage current occurs, leading to dielectric breakdown and sample damage at high voltages. Additionally, ferroelectric sample domains will flip (pole) if the coercive voltage is exceeded by the AC voltage. At this point, the measured amplitude will no longer reflect a purely piezoelectric response and the hysteresis loop will begin to collapse. For thin films, the nucleation voltage is often <5 V, significantly limiting the practical AC amplitude.

2. Increase the amplification of the deflection signal

A second approach to improving PFM signal levels is to increase the amplification. Amplification eliminates bit-noise, but the signal-to-noise ratio (SNR) is only slightly improved. Signal amplification (by a factor of 16) is available to all Dimension Icon® users by choosing the "Optimized Vertical" or "Vx16" workspace.

3. Increase the time constant of the lock-in amplifier

Increasing the lock-in amplifier's time constant increases averaging, thereby decreasing noise. This noise reduction comes at the cost in update time, resulting in slower data acquisition, but is worth considering for low-response samples.

4. Amplify the PFM motion mechanically

PFM vibration can be mechanically amplified by using the cantilever contact resonance. This method, known as contact resonance PFM (CR-PFM), can provide a significant (as much as 100x) boost to PFM sensitivity, allowing detection of amplitudes down to <1 pm, but adding an element of complexity.

Quantification of the CR-PFM amplitude requires calculation of the *CR shape factor* from the contact resonance frequency, amplitude, and quality factor (Q).[6] CR-PFM measurements can be collected at fixed frequency or by using a resonance tracking method, such as frequency sweeps, dual-frequency resonance tracking (DFRT), or band excitation (BE). Since the CR frequency usually shifts during scanning, fixed-frequency measurements near resonance are not recommended for quantitative PFM. Instead, it is preferred to use Ramp, RampScript, or force volume (FV)-based methods that can precisely control the forces while collecting detailed frequency spectra.

Improving Repeatability with DataCube Methods

DataCube (DCUBE) CR-PFM is a FV-based hyperspectral imaging technique that provides maps of CR-PFM amplitude with associated frequency, *Q* factor, and phase on resonance. Figure 2 provides example DCUBE CR-PFM results collected on a PMN-PT sample to demonstrate how the method works:

1. At each pixel in the image, a force curve is collected with a surface hold segment (Figure 2a).
2. During the hold segment the frequency of the AC stimulation voltage is swept over a user specified range while collecting deflection amplitude and phase spectra (Figures 2b and 2c respectively).
3. Spectra are analyzed and used to create maps of sample properties over the scan area (Figures 2d-f).

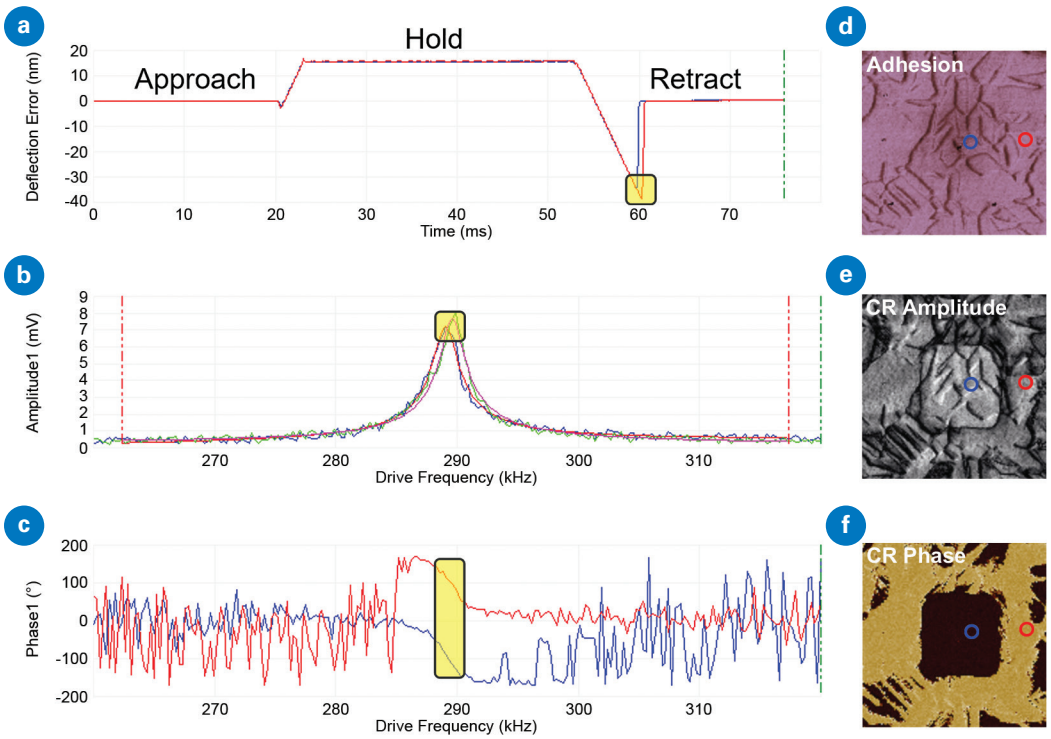

FIGURE 2

DataCube (DCUBE) CR-PFM of a PMN-PT ferroelectric sample: (a) Typical force vs. time plots showing 30 ms hold segments where frequency is swept and highlighted pull-off points for adhesion map, (b) PFM Amplitude spectra from hold segment and Lorentzian fits used to calculate CR Amplitude (peaks highlighted), Frequency, and *Q*, (c) PFM Phase spectra used to determine CR Phase (region of CR highlighted), (d) Adhesion map with approximate locations of curves in (a), (e) CR Amplitude map with locations of curves in (b), and (f) CR Phase map with locations of curves in (c).

It is important to note that the usual force curve approach and retract data is available along with the hold segment, so it is possible to do the usual fitting and obtain maps of mechanical properties such as modulus and adhesion (Figure 2d) from the same dataset.

Since duration, sweep width, and sampling rate of the hold segment are user-controlled, the CR-PFM maps can be optimized for accuracy and SNR. Figure 2b shows how two typical CR-PFM spectra are fit to generate maps of CR Amplitude (Figure 2e). Once the precise CR frequency is known, the CR Phase can be obtained (Figure 2c) and the associated map generated (Figure 2f). The contact resonance frequency, amplitude, and *Q* are defined by fitting hundreds of points, allowing for improved accuracy over dual-frequency resonance tracking (DFRT)-based methods – especially for *Q*. Additionally, long integration times (increased lock-in time constants) are possible when longer hold times are acceptable. If multiple CR eigenmodes are of interest, they can be collected in a single pass by simply increasing the frequency sweep width (though some care is required to avoid distorting the resonance peaks by sweeping too quickly).

Because DCUBE methods are based on FV, the tip is not dragging on the surface between measurements, which eliminates the lateral force that occurs in contact mode and often damages samples and probes. Thus, the tip apex is preserved, resulting in more consistent measurements than comparable contact mode techniques. DCUBE also enables measurements on samples that are susceptible to damage or displacement by the AFM tip dragging across the surface, like nanoribbons and fibers. Softer cantilevers can partially mitigate this issue but are more prone to electrostatic artifacts than stiffer cantilevers – more on this later.

Phase Considerations

For reliable PFM results, it is necessary to compensate for any instrument-induced phase shift. Digital lock-ins have a fixed time delay for processing data. As the frequency increases, this fixed time delay leads to an approximately linear increasing phase shift. Since the shift varies relatively slowly with frequency (Figure 3a: ~0.4°/kHz), a simple subtraction of an *offset phase* is generally sufficient to compensate for the issue.[7] When working with the same type of probe, the needed *offset phase* will be very similar because the cantilever resonance frequencies are similar. However, any change to signal path, including microscope cable length, may change the phase shift. If the instrumental phase shift is not compensated, this can lead to an inversion of the PFM hysteresis loops (Figure 3c).

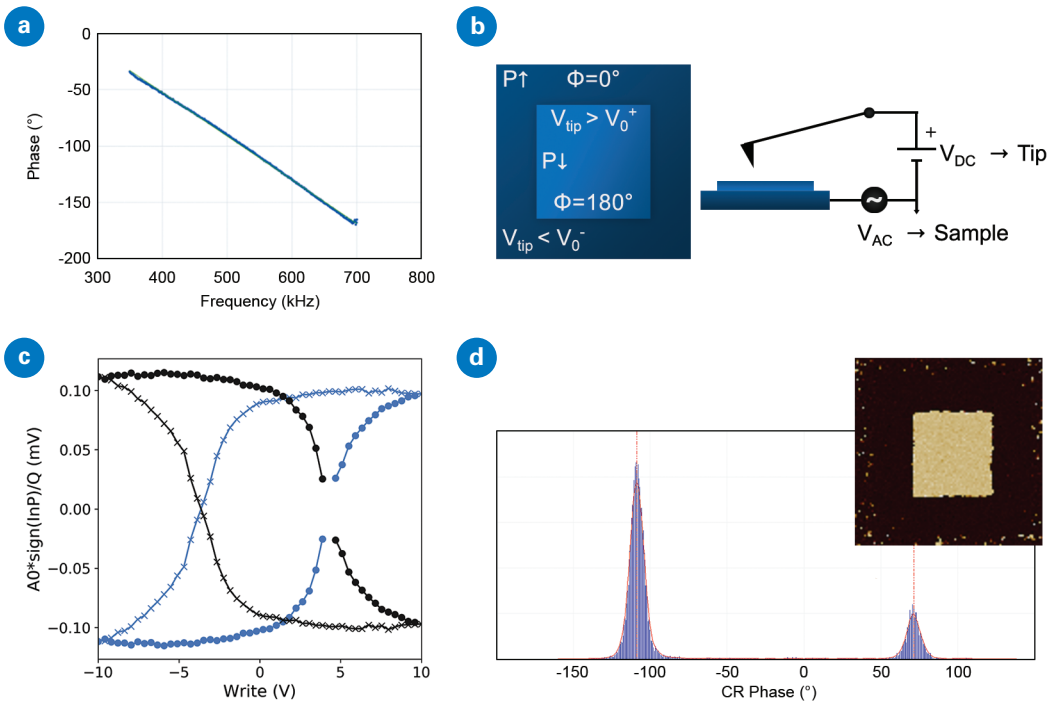

FIGURE 3

Compensating for instrumental phase shifts: (a) the measured phase from the lock-in depends approximately linearly on frequency, with a phase shift of about -4 deg/kHz, (b) domain polarization and expected phase after applying negative and positive DC tip voltages to pole concentric domains in a ferroelectric sample with known positive electrostrictive coefficient, (c) if this phase shift is not compensated, the direction of ferroelectric hysteresis loops may be inverted when probes of different frequencies are used, and (d) histogram of phase data from a DCUBE CR-PFM map (inset) after poling with pattern in (b) has peaks at -109° (outer domain) and +71°.

To determine the phase shift at a given frequency, we follow the method of Neumayer et al.[7] in using a reference ferroelectric sample to first create and then measure domains of known orientation. Materials like PZT and PMN-PT are known to have positive electrostrictive coefficients, so an increasing electric field applied in parallel to the polarization of a domain in the material will result in an expansion of the material. By applying a sufficiently large negative voltage to the tip (electric field up), it is possible to flip the domain polarization up. One can then pole and measure two concentric squares (Figure 3b):

1. negative DC voltage ($<V_0^-$) to the tip for the outer square
2. positive DC voltage ($>V_0^+$) to the tip for the inner square
3. set DC voltage to zero and scan the area to measure the PFM phase

When the AC voltage is applied to the sample, the outer square should have phase of 0° (inner at 180°). However, the lock-in phase range is ±180°, so the inner domain will tend to wrap (noise causing the phase to jump between +180° and -180°). To avoid this wrapping, it is generally preferable to adjust a lock-in parameter called the *drive phase* to make the outer domain +90° (inner at -90°): if this is done the -90° should be added back to the data during analysis. In Figure 3d, a Bruker SCM-PIT-V2 probe was used with free resonance frequency 62.7 kHz (CR frequency 282 kHz). The outer domain had a mean value of -109° (with lock-in *drive phase* of 0°), so subsequent data was collected with a lock-in *drive phase* of +90° + 109° -0° = -161°. The resulting hysteresis loops have the expected clockwise direction.

Electrostatic Signal

One of the biggest challenges for researchers looking to quantify their PFM measurements is the influence of electrostatic forces from the sample acting on the entire length of the cantilever (Figure 4a). This electrostatic signal is proportional the contact potential difference (CPD) between tip and sample and adds linearly to the piezoelectric response of the material. When charge injection from the tip changes the CPD, this phenomenon can result in non-ferroelectric materials exhibiting a PFM response that is very similar to a ferroelectric, even exhibiting the classic hysteresis loops and butterfly amplitude loops.[5]

To understand and begin to decouple this electrostatic signal from the piezoelectric signal, one or more of a few approaches is generally used, each with advantages and disadvantages:

Increase the cantilever stiffness

Under the same electrostatic force, stiffer cantilevers bend less, leading to a smaller contribution from the electrostatic signal (in contrast, the piezoelectric response is not sensitive to the cantilever stiffness except for very soft samples). This has recently been verified for sub-resonance PFM, where the electrostatic contribution was less than that of the piezoelectric contribution for spring constant (k_c) over about 25 N/m on periodically poled lithium niobate (PPLN).[8]

Unfortunately, tip wear and sample damage can occur with very stiff probes in contact mode. Cantilevers softer than k_c=10 N/m are usually preferred for all but low-resolution PFM measurements on stiff samples. However, with DCUBE PFM and SS-PFM, the uncontrolled lateral forces that occur in contact mode are avoided, enabling the use of relatively stiff probes with minimal damage to tip or sample.

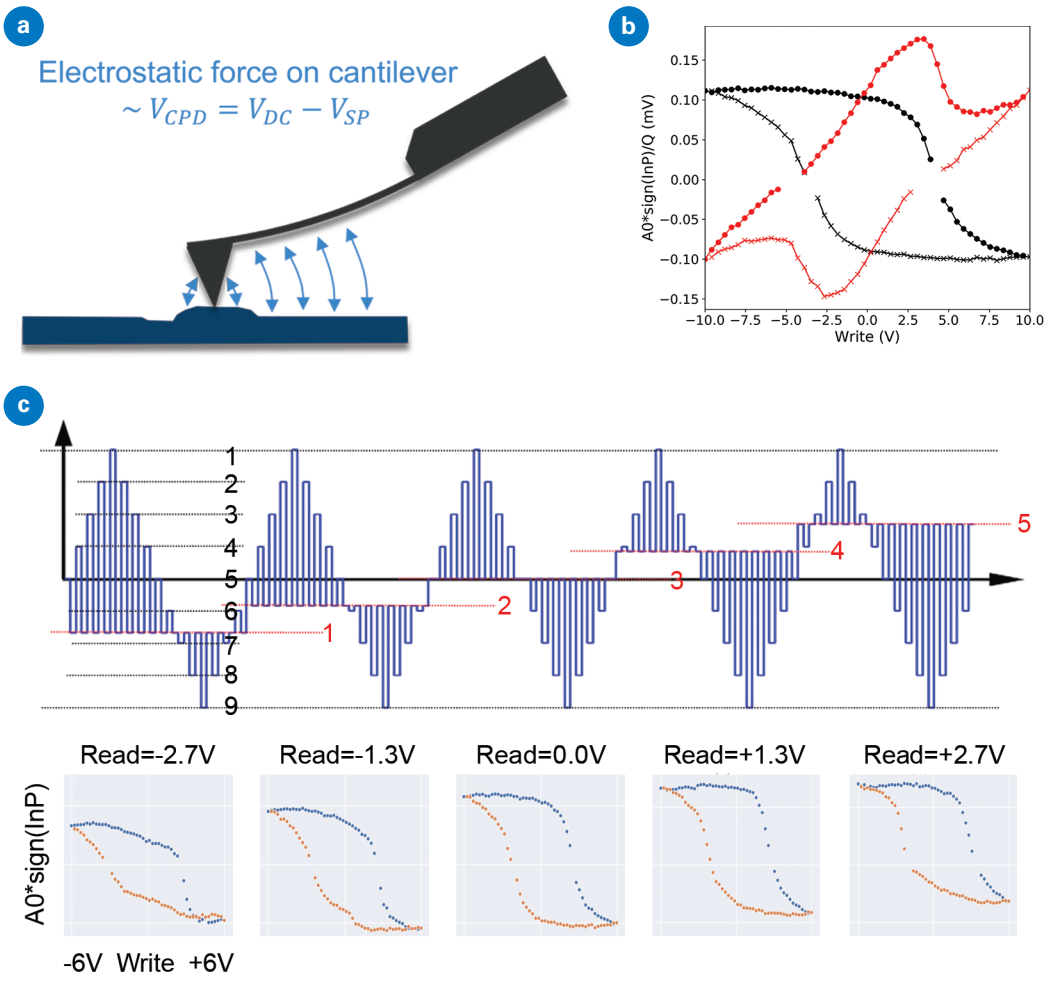

FIGURE 4

Understanding the influence of electrostatics on the PFM response: (a) the electrostatic force on the cantilever is proportional to the contact potential difference or the difference between the applied voltage (V_{DC}) and the surface potential (V_{SP}), (b) comparing PFM hysteresis loops collected during read segments (black) and write segments (red) can be used to discriminate between ferroelectric and non-ferroelectric materials, and (c) by measuring SS-PFM hysteresis loops (bottom) at different read voltages (top) it is possible to directly study the influence of varying contact potential difference on PFM measurements.

Use SS-PFM to investigate bias dependence

Another approach is to use an applied DC bias during SS-PFM spectroscopy to investigate changes in electrostatic forces that occur after charge injection. Bruker's SS-PFM implementation allows this to be done in two different ways: [5]

1. Comparing the hysteresis loops with measurements acquired during the read segments (at zero bias) with those acquired during the write segments (at a range of voltages)
2. Sequentially performing the SS-PFM measurements at multiple different read voltages

Figure 4b is an example of the first method, showing PFM response for the off-field (0 V read segments) and on-field (write segments). Note that the on-field case looks very similar to the off-field case, except that it is tilted due to the electrostatic force on the cantilever from the DC voltage that is applied during the write segments. For a non-ferroelectric material, the tilt remains, but there is little or no hysteresis in the on-field loop, and loop direction may change. Figure 4c (top) shows a schematic of the DC voltage applied during the second method with five different read voltages. It is clear (Figure 4c bottom) that doing the SS-PFM at different read voltages changes the shape and shifts the position of the hysteresis loop as if the surface potential had changed. The effect of the combined (constant) ferroelectric and (linear) electrostatic response, i.e., $\frac{D_{AC}}{V_{AC}} = d_{33} + \frac{1}{k^*}\frac{dC}{dz}(V_{DC} - V_{SP})$ is shown schematically in Figure 5a.[6]

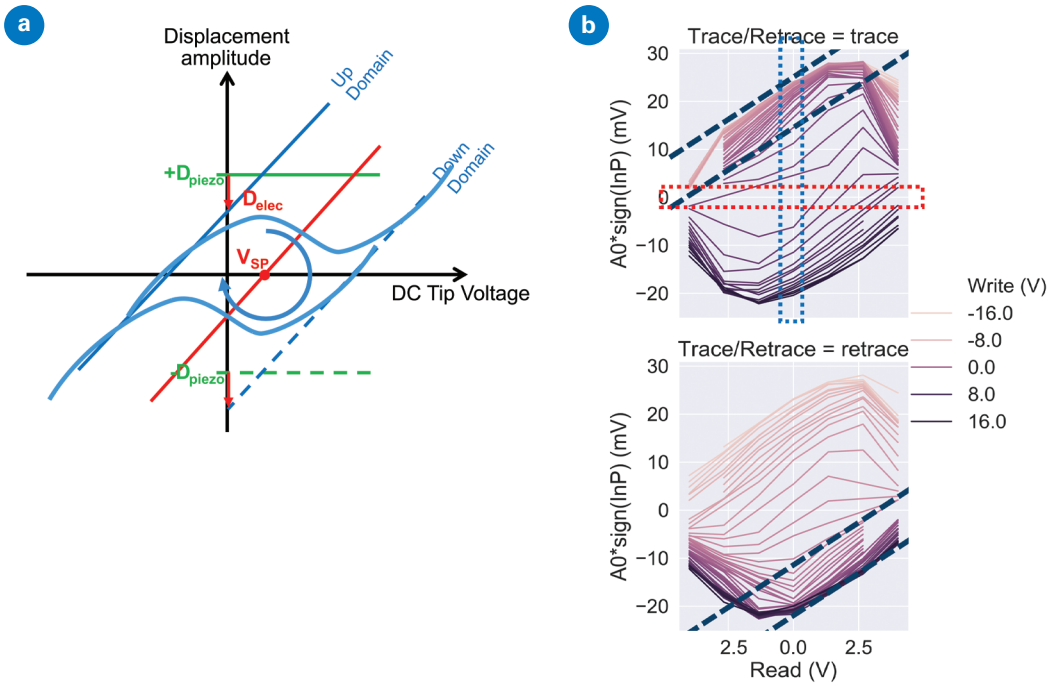

FIGURE 5

PFM response with applied bias on ferroelectric samples: (a) schematic of ferroelectric hysteresis without electrostatics (green), with electrostatics on a non-ferroelectric sample (red), and with both electrostatics and ferroelectric behavior (blue). (b) cKPFM plots from a ferroelectric material at different write voltages. The dashed black lines indicate the electrostatic response in the part of the hysteresis curve where the ferroelectric response of the sample is saturated. If the sample were an ideal dielectric, the red dashed box would indicate the surface potential for the sample which changes from one write voltage to the next due to charge injection from the tip. The blue dashed box indicates the PFM response for the off-field hysteresis loop. Data is from a PZT sample with DC voltage applied to tip, AC to sample.

Plotting the response data for each write bias is as a function of read bias results in a cKPFM plot.[5] Figure 5b shows a cKPFM plot of data collected on a ferroelectric (PZT). The electrostatic response is indicated by the tilt in the linear parts of the curve at the extremes of write bias (where the ferroelectric response is saturated: black dashed lines). In contrast, the non-linearity in the cKPFM plots indicate ferroelectric response. For an ideal dielectric material, all plots would be linear, with the x-intercepts (red box in Figure 5b) indicating the surface potential for the sample after charge injection by the associated write segment. Similarly, the y-intercepts (blue box) indicate the PFM response for the off-field hysteresis loop.

For ferroelectric materials, it is difficult to separate the electrostatic and ferroelectric response because the surface potential (and therefore the electrostatic contribution to displacement) changes from one write segment to the next. Therefore, even if one of the read voltages precisely cancels out the surface potential at the beginning of the measurement, it cannot do so for the whole hysteresis loop. To address this, Balke et al. used a combination of on-field SS-PFM (for PFM response and electrostatic slope) and non-contact KPFM (for surface potential) with the same write waveform.[6] This worked well for PPLN with DC voltages below the coercive voltage (avoiding domain switching), but does not allow correction of the entire hysteresis loop.

Position the beam-bounce laser at the electrostatic blind spot

A third approach involves using sub-resonance PFM and carefully positioning the beam-bounce laser used to detect the cantilever deflection angle at the electrostatic blind spot (ESBS) for the lever.[9] The ESBS is the location at which the distributed electrostatic force on the cantilever does not influence its slope and as a result does not affect the deflection measured by the AFM.

This ESBS method works well with both stiff and soft cantilevers but does not work for CR-PFM, where the cantilever shape is dominated by contact resonance behavior. For frequencies well below contact resonance, the relative contribution of the electrostatic force to the slope of the cantilever depends on where along the cantilever it is measured. For most cantilevers, the ESBS is located at about 2/3 of the way from the base of the cantilever to the tip, though the precise position depends on the contact stiffness.

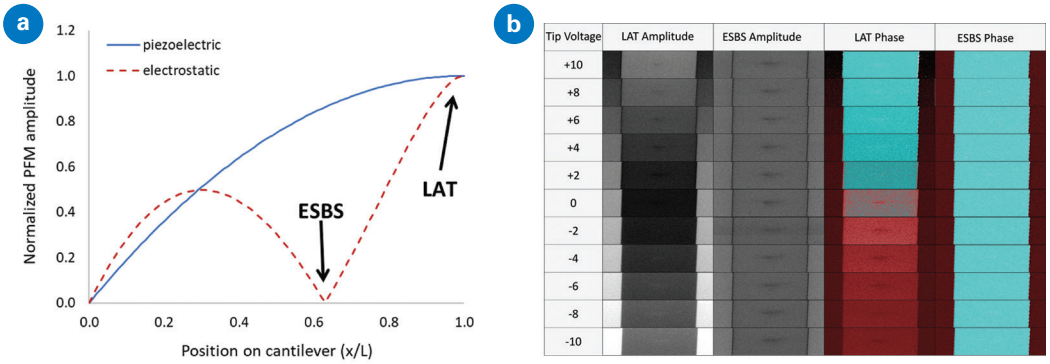

FIGURE 6

The effect of electrostatic force on the cantilever depends on beam-bounce laser position: (a) the electrostatic force on the cantilever has minimal influence on the cantilever deflection when the laser is positioned at the electrostatic blind spot (ESBS, see red-dashed line), (b) PFM maps of amplitude (left) and phase (right) collected at different tip voltages on PPLN demonstrate the significant variation in response with surface potential when the laser is positioned at the tip (LAT) and the improvement possible with the ESBS.

Figure 6a illustrates the effects of pure tip displacement (piezoelectric) and distributed force on the cantilever (electrostatic) bending of the cantilever. PFM is sensitive to the sum of the slope from both sources, so positioning the laser at the ESBS will result in significantly less electrostatic artifact than the usual laser at tip (LAT) position. For best performance, the laser position is iteratively adjusted until one of the following occurs:

- $Amp|_{\uparrow domain} = Amp|_{\downarrow domain}$ for a sample where this is expected (like PPLN);
- Amp is minimized on a non-piezoelectric sample;
- $\partial Amp/\partial V_{DC}$ is minimized.

Figure 6b compares PFM images collected on PPLN at different tip voltages using a Bruker SCM-PIT-V2 probe with spring constant k_c = 2.7 N/m. The leftmost two columns compare PFM amplitudes with LAT and at the ESBS, while the rightmost columns compare PFM phase. As expected, the ESBS amplitude of the center domain matches the outer domains across tip voltages from -10 V to +10 V, but there is a wide range of amplitude for LAT. Likewise, the ESBS phase is very consistent over the voltage range, but not so for LAT. Quantifying this for the ESBS case, we find d_{33}=9.3±0.3 pm/V for the center domain and 10.7±0.9 pm/V for the left domain. Placing the laser at the end (LAT) results in d_{33}=5.9±2.8 pm/V for the center domain and 12.4±6.6 pm/V for the left domain – more than a factor of two difference. The difference is even more extreme in the phase channel – for ESBS the phase difference between domains ranges from +178.1° to +179.9° (where the expected value is +180°). In contrast, the LAT phase difference ranges from -15.3° to +201.4°. These results demonstrate that, by simply positioning the laser at the ESBS, the electrostatic component of the PFM signal is nearly completely eliminated.

Combining SS-PFM with sub-resonance PFM at either LAT or ESBS, the influence of imposed electrostatics can be examined (via the read bias) on PFM spectra. Figure 7 shows PFM amplitude 'butterfly loops' on a PZT thin film with write voltages from -11 V to +11 V. To see the influence of the electrostatic force on the measurements, the read voltages were also varied from -2.7 to +2.7 V. In Figure 7a (LAT), only the loop for read (0 V) has the usual symmetric loop. All the others are skewed one way or the other. In contrast, Figure 7b (laser at ESBS) produced loops that are reasonably consistent up to ±1.8 V.

FIGURE 7

Investigating the influence of beam-bounce laser position on PFM response using sub-resonance SS-PFM; (a) PFM amplitude vs. write voltage spectra ('butterfly loops') at different read voltages with laser positioned near the end of the cantilever (LAT). (b) PFM spectra at different read voltages with laser positioned at the electrostatic blind spot (ESBS).

Sample: PZT
Probe: SCM-PIT-V2

Mapping ferroelectric parameters

If spectroscopy is conducted at multiple positions across a surface, a map of any parameter from the hysteresis loop can be generated.[10] In Figure 8a, a single piezoelectric loop (top) is analyzed to obtain ferroelectric parameter at one point. This is repeated for every point in a 20x20 array, and maps of coercive voltages V_0^+ and V_0^- are generated (bottom). The mapping is done using MIROView™, allowing the array to be co-located with other AFM measurements (topography, adhesion, dissipation, elastic modulus, etc.), previously poled regions, or optical images. Figure 8b correlates a CR-PFM phase image collected after the spectroscopic map showing poled regions with the positive coercive bias by overlaying a map of contour lines with constant V_0^+. This type of correlation can be used to understand the influence of nanostructures like grain boundaries and defects on the ferroelectric behavior of the material.

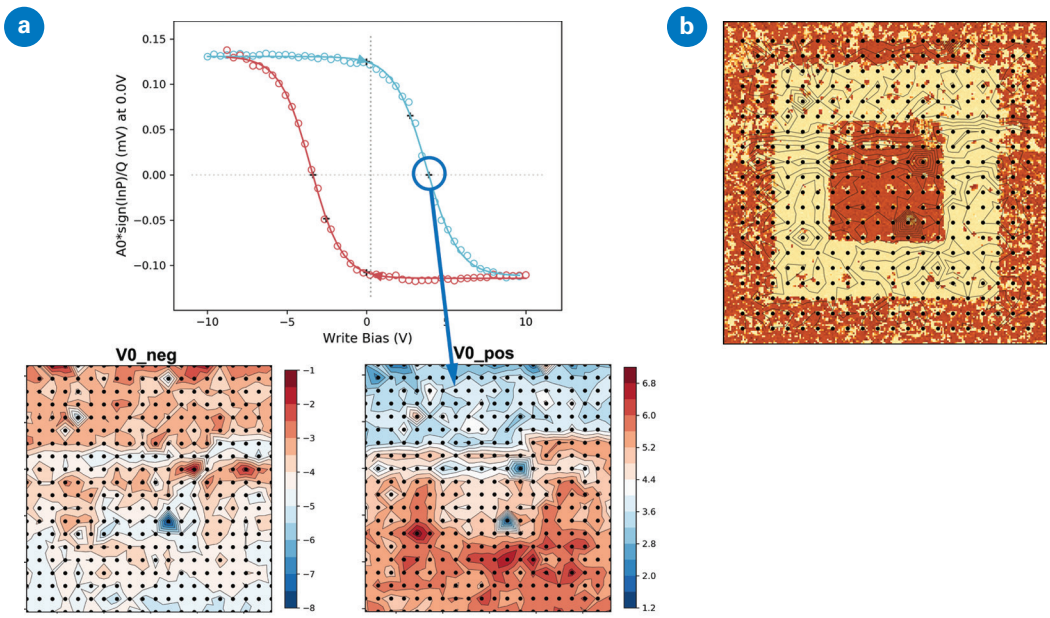

FIGURE 8

Maps of ferroelectric properties can be extracted from arrays of spectra: (a) top is a ferroelectric hysteresis loop from resonant SS-PFM on PZT, in (a) bottom key parameters such as coercive voltages V_0^+ and V_0^- are extracted from the loops and mapped; (b) V_0^+ map is overlaid upon a subsequent PFM phase map to look for influence of domain structure on coercive voltages.

If desired, PeakForce Tapping® can be used to find the region of interest instead of contact mode, protecting the tip even further and avoiding damage to even the most delicate samples. If high levels of detail are required, MIROView supports arrays of up to 50x50 = 2500 spectra of 10 to 20 MB each, resulting in a full data set of 25 to 50 GB. Collecting such large data sets takes time, but Bruker's DSP-based RampScripting minimizes the total acquisition time by eliminating system latencies between different segments in the script (switching times are on the order of 10 µs).

Conclusions

While there are several challenges regarding collecting and analyzing quality PFM data, the resolution and sensitivity of the AFM make it a compelling choice for investigating ferroelectric materials. If care is taken to compensate for electrostatics and instrumental artifacts, results can be compared across different labs and types of instruments and development of structure-property relationships are facilitated.

Bruker's DCUBE PFM and SS-PFM both work with either contact resonance or sub-resonance PFM and can be used with PeakForce Tapping for survey scanning, eliminating contact mode and its attendant lateral forces. They thereby provide more repeatable results, enable interrogation of delicate samples, and allow for use of stiffer levers, lessening electrostatic artifacts.

Key practical solutions

- If sample response is weak or coercive voltages are low, contact resonance is recommended to maximize signal to noise, but careful analysis is needed for quantification of response amplitude. When sample response is stronger, sub-resonance PFM is the most direct way to obtain quantitative amplitude data (and d_{33}).
- By poling a sample with known electrostrictive coefficient sign, it is possible to calibrate the system phase offset at a given frequency, allowing correct interpretation of spectroscopic data.
- The electrostatic force on the cantilever can induce a PFM artifact that is very similar to the ferroelectric response. For sub-resonance PFM this can be mitigated by positioning the beam bounce laser at the electrostatic blind spot on the cantilever.
- SS-PFM can be used to investigate the influence of electrostatics on the PFM spectra for both resonance and sub-resonance PFM using varying read voltages.
- Arrays of SS-PFM spectra can be analyzed and used to generate maps of key ferroelectric parameters, enabling correlation with nanostructures at the sample surface.

Acknowledgements

We thank Jason Killgore (NIST) and Liam Collins (ORNL) for many useful discussions and clarifications, which significantly improved this document.

References

1. Kalinin, S. v., Rodriguez, B. J., Jesse, S., Shin, J., Baddorf, A. P., Gupta, P., Jain, H., Williams, D. B., & Gruverman, A. (2006). Vector Piezoresponse Force Microscopy. *Microscopy and Microanalysis, 12*(03), 206–220. https://doi.org/10.1017/S1431927606060156
2. Hidaka, T., Maruyama, T., Saitoh, M., Mikoshiba, N., Shimizu, M., Shiosaki, T., Wills, L. A., Hiskes, R., Dicarolis, S. A., & Amano, J. (1996). Formation and observation of 50 nm polarized domains in $PbZr_{1-x}Ti_xO_3$ thin film using scanning probe microscope. *Applied Physics Letters, 68*(17), 2358–2359. https://doi.org/10.1063/1.115857
3. Jesse, S., Baddorf, A. P., & Kalinin, S. v. (2006). Switching spectroscopy piezoresponse force microscopy of ferroelectric materials. *Applied Physics Letters, 88*(6), 062908. https://doi.org/10.1063/1.2172216
4. Vasudevan, R. K., Balke, N., Maksymovych, P., Jesse, S., & Kalinin, S. v. (2017). Ferroelectric or non-ferroelectric: Why so many materials exhibit "ferroelectricity" on the nanoscale. *Applied Physics Reviews, 4*(2), 021302. https://doi.org/10.1063/1.4979015
5. Balke, N., Maksymovych, P., Jesse, S., Herklotz, A., Tselev, A., Eom, C.-B., Kravchenko, I. I., Yu, P., & Kalinin, S. v. (2015). Differentiating Ferroelectric and Nonferroelectric Electromechanical Effects with Scanning Probe Microscopy. *ACS Nano, 9*(6), 6484–6492. https://doi.org/10.1021/acsnano.5b02227
6. Balke, N., Jesse, S., Yu, P., ben Carmichael, Kalinin, S. v, & Tselev, A. (2016). Quantification of surface displacements and electromechanical phenomena via dynamic atomic force microscopy. *Nanotechnology, 27*(42), 425707. https://doi.org/10.1088/0957-4484/27/42/425707
7. Neumayer, S. M., Saremi, S., Martin, L. W., Collins, L., Tselev, A., Jesse, S., Kalinin, S. v., & Balke, N. (2020). Piezoresponse amplitude and phase quantified for electromechanical characterization. *Journal of Applied Physics, 128*(17), 171105. https://doi.org/10.1063/5.0011631
8. Kim, S., Seol, D., Lu, X., Alexe, M., & Kim, Y. (2017). Electrostatic-free piezoresponse force microscopy. *Scientific Reports, 7*(1), 41657. https://doi.org/10.1038/srep41657
9. Killgore, J. P., Robins, L., & Collins, L. (2022). Electrostatically-blind quantitative piezoresponse force microscopy free of distributed-force artifacts. *Nanoscale Advances, 4*(8), 2036–2045. https://doi.org/10.1039/D2NA00046F
10. Jesse, S., Lee, H. N., & Kalinin, S. v. (2006). Quantitative mapping of switching behavior in piezoresponse force microscopy. *Review of Scientific Instruments, 77*(7), 073702. https://doi.org/10.1063/1.2214699

Bruker Nano Surfaces and Metrology

Santa Barbara, CA • USA
Phone +1.805.767.1400

productinfo@bruker.com

www.bruker.com/AFM